ACS APPLIED MATERIALS & INTERFACES

Research Article

www.acsami.org

Robust Composite-Shell Microcapsules via Pickering Emulsification

Marcia W. Patchan, Benedict W. Fuller, Lance M. Baird, Paul K. Gong, Erich C. Walter, Brendan J. Vidmar, Ike Kyei, Zhiyong Xia, and Jason J. Benkoski*

The Johns Hopkins University Applied Physics Laboratory, 11100 Johns Hopkins Road, Laurel, Maryland 20723, United States

Supporting Information

ABSTRACT: Microencapsulation technology has been increasingly applied toward the development of self-healing paints. Added to paint as a dry powder prior to spraying, the microcapsules store a liquid that can repair the protective barrier layer if released into a scratch. However, self-healing will not occur unless the microcapsules can withstand spray-painting, aggressive solvents in the paint, and long-term exposure to the elements. We have therefore developed a one-pot synthesis for the production of Pickering microcapsules with outstanding strength, solvent resistance, and barrier properties. Octadecyltrimethoxysilane-filled (OTS) microcapsules form via standard interfacial polycondensation, except that silica nanopowder (10−20 nm diameter) replaces the conventional surfactant or hydrocolloid emulsifier. Isophorone diisocyanate (IPDI) in the OTS core reacts with diethylenetriamine, polyethylenimine, and water to form a hard polymer shell along the interface. Compared to pure polyurea, the silica-polyurea composite improves the shelf life of the OTS by 10 times. The addition of SiO_2 prevents leaching of OTS into xylenes and hexanes for up to 80 days, and the resulting microcapsules survive nebulization through a spray gun at 620 kPa in a 500 cSt fluid.

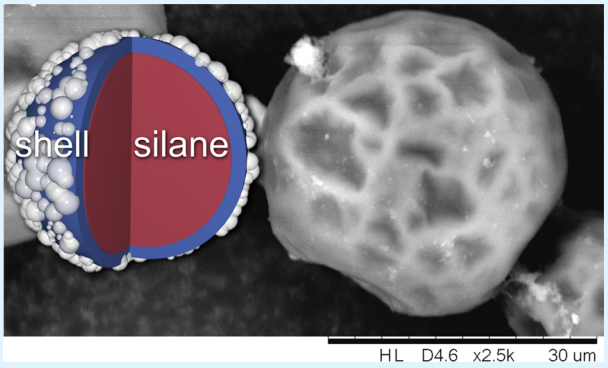

KEYWORDS: *microencapsulation, pickering emulsion, interfacial polymerization, hydrolysis, solvent resistance*

INTRODUCTION

Microcapsules are microscopic, hollow spheres filled with an active liquid ingredient. They find wide use in a number of specialty chemical products, including pesticides,[1,2] fragrances,[3] carbonless paper,[4] personal care products,[5] and pharmaceuticals.[6,7] Their popularity stems from their core capability: controlling the release of the active ingredient. Controlled release comes in the form of a polymer or inorganic shell, which can release its contents in one of three ways: constant permeability, environmentally controlled permeability, or triggered release. For microcapsules with fixed permeability, small molecules diffuse through a permeable membrane or porous shell to achieve a controlled release profile for an extended time.[8,9] The second possibility is an outer shell that gradually dissolves or degrades in response to environmental conditions. Solvents, caustics, enzymes, pH, moisture, irradiation, or other environmental factors thus regulate the rate of release.[10−12] A third possibility is sudden rupture in response to an external stimulus. Examples include ultrasonication,[13,14] heating,[15,16] light,[17] and solvents.[18]

The focus of the current study is to develop a mechano-responsive microcapsule for self-healing paints, which have extreme requirements for high strength and low permeability. In this application, microcapsules are added to the paint prior to spraying. Once the paint dries, the microcapsules store a small reservoir of liquid corrosion inhibitor that remains latent until needed. When the coating sustains damage, the microcapsules rupture, and the inhibitor flows into the scratch, where it forms a protective layer over the freshly exposed metal.

Although the microcapsules must break when scratched, they must also be strong enough to prevent premature rupture during stirring, filtration, scraping, sieving, pouring, fluidization, and spraying from viscous media. Even a small fraction of broken microcapsules can have catastrophic effects on dispersion in the paint or adhesion, so it should be avoided at all costs. Unfortunately, polymer microcapsules are inherently fragile due to their thin walls. Compared to metals and ceramics, they have relatively modest elastic moduli on the order of 1 GPa, and tensile strengths on the order of only 50 MPa.[19] Our goal, then, is to develop a synthesis strategy that preserves the scalability and low cost of polymer microcapsule synthesis yet achieves sufficient strength in a micron-thick shell to safely meet the requirements of this application.

The microcapsule should be strong but not so strong that it does not break during scratching. Fortunately, the paint bears the vast majority of the load by virtue of its greater thickness relative to the microcapsule shell (100 μm versus 1 μm). What results, then, is a situation where the microcapsule almost cannot be too strong. Provided that the adhesion of the microcapsule to the paint exceeds the cohesive strength of the

Received: January 19, 2015
Accepted: March 19, 2015
Published: March 19, 2015

DOI: 10.1021/acsami.5b00494
ACS Appl. Mater. Interfaces 2015, 7, 7315−7323

Scheme 1. Chemical Structures for Compounds Comprising (A) OTS/IPDI/SiO_2 Microcapsules and (B) DTS/BCI/GA Microcapsules

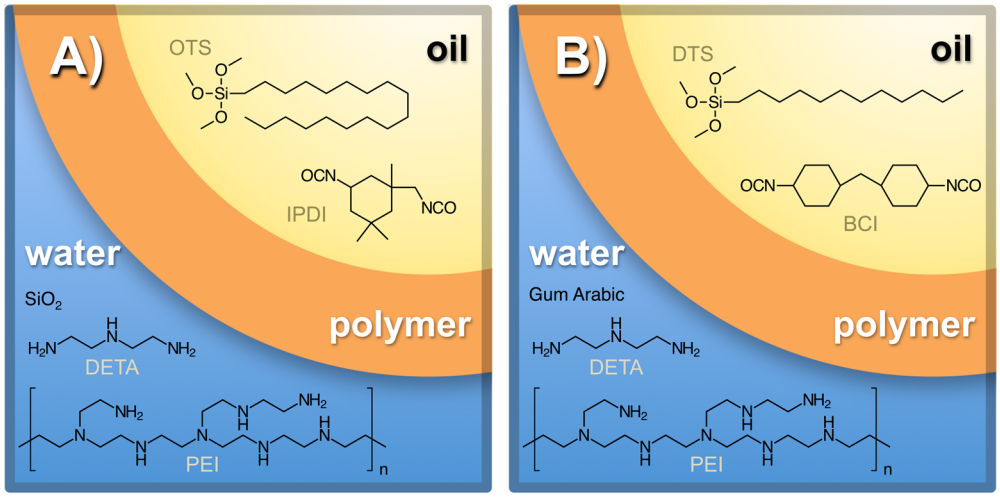

microcapsule shell, damage to the paint virtually assures microcapsule rupture.

Also unique to this application are the requirements for protecting the active ingredient; paints remain in service for many years, and thus, the active ingredient must not degrade over an extensive time span. Paints also include a variety of solvents and reactive chemicals that can degrade or compromise the microcapsule shell before the paint is applied. So, whether subjected to hydrolysis, oxidation, or solvent leaching, the thin microcapsule membrane must come as close to a hermetic seal as possible. Polymer microcapsules also struggle to meet this requirement because of their relatively high permeability to water, oxygen, and small organic molecules.[20,21] As such, a polymer microcapsule shell cannot be counted on to protect chemically active species from oxidation, leaching, or hydrolytic attack indefinitely.

Herein, we present a facile synthetic method for improving the strength and barrier properties of polymer microcapsules. The key is to use silica nanopowder to form a Pickering emulsion rather than relying upon surfactants or hydrocolloids to stabilize the initial emulsion. The nanoparticles remain embedded at the interface following interfacial polycondensation, resulting in a silica-reinforced polyurea shell. Because the silica nanopowder is completely consumed in the reaction, this approach avoids complications that can result when surfactants or hydrocolloids leave residues behind on the surface.

Pickering emulsions employ the use of interfacially active solid particles to increase the stability of the emulsion through steric repulsion. Additionally, the incorporation of the solid particles into the resulting microcapsule shell provides further benefits to mechanical strength, solvent resistance, and barrier properties. A wide range of particles, including magnetic particles,[22] clays,[23,24] and polymers,[25] has been applied for synthesis of Pickering emulsions. Silica is a popular stabilizing particle in part because the particle surface can be easily modified to control hydrophobicity, but also because the particle−particle interactions at the interface bring about additional stabilization.[26] Accordingly, microcapsules synthesized from silica-based Pickering emulsions have shown improved shell properties.[27−29]

In this study, we investigate the effects of the emulsifier, shell-forming monomer and interior solvent quality on the microcapsule physical properties, which include shelf life, solvent resistance, and mechanical durability. Specifically, we measure the rate of hydrolytic degradation of octadecyltrimethoxysilane (OTS) within the microcapsules under ambient conditions, the rate of OTS release from the microcapsules into organic solvents, and the resistance of the microcapsules to rupture under shear.

EXPERIMENTAL SECTION

Reagents. All reagents were purchased from Sigma-Aldrich and used without further purification unless otherwise noted. Isophorone diisocyanate (CAS [4098-71-9]), poly(ethylenimine) 50% (aq) (CAS [9002-98-6]; Mn ~60 000), Gum Arabic (CAS [9000-01-5]), diethylenetriamine (CAS [111-40-0]), *n*-octadecyl trimethoxysilane (Gelest, CAS [3069-42-9]), silicon dioxide (CAS [7631-86-9]), 4,4′-methylenebis(cyclohexylisocyanate) (CAS [5124-301-1]), dodecyl trimethoxysilane (Gelest, CAS [3069-21-4]).

Microcapsule Synthesis. Oil-in-water emulsification accompanied by interfacial polymerization afforded spherical microcapsules with a liquid interior and thin polymer shell. An IKA rotar-stator (Model No. T25) vortexed the solution. The oil phase was prepared from a 35:65 (w/w) mixture of isophorone diisocyanate (IPDI) and OTS. The aqueous phase consisted of either a 5% (w/v) aqueous Gum Arabic (GA) solution or a 5% (w/v) SiO_2 nanoparticle suspension. The cross-linker solution contained a mixture of the water-soluble cross-linkers, diethylenetriamine (DETA) and polyethylenimine (PEI) at 5% (w/v) each in either the 5% (w/v) aqueous Gum Arabic (GA) or pure water.

First, 20 g of monomer mixture were placed into 80 mL of the water phase solution and stirred at 8000 rpm using the IKA mixer for 10 min. Then, 20 g of cross-linker solution was added to the mixture, stirred for 5 min, and allowed to incubate in water for a fixed time at a fixed temperature. The following incubation conditions were tested: 4 days at 25 °C, 4 days at 60 °C, and 1 day at 90 °C. Note that some formulations did not produce stable microcapsules under all three conditions due to the large differences in emulsion stability and reaction kinetics. Following incubation, the supernatant liquid was decanted and the microcapsules were washed three times with Milli-Q water. The reaction yielded 20 g of microcapsules. To examine the effect of silane polarity, we substituted dodecyl trimethoxysilane (DTS) for OTS. To examine the effect of polymer shell composition, 4,4′-methylenebis(cyclohexylisocyanate) (BCI) was substituted for IPDI.

Unless otherwise noted, the microcapsules will be referred to using the following notation: fill/monomer/emulsifier. For example, OTS/IPDI/SiO_2 refers to OTS-filled microcapsules with an IPDI shell and a

DOI: 10.1021/acsami.5b00494
ACS Appl. Mater. Interfaces 2015, 7, 7315−7323

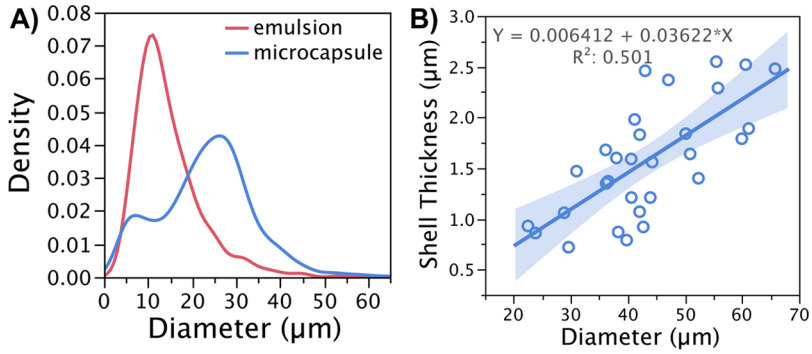

Figure 1. A) Typical microcapsule size distribution for OTS/IPDI/SiO_2 microcapsules synthesized at 90 °C and the corresponding emulsion. B) Microcapsule shell thickness plotted as a function of diameter for a population of 30 microcapsules. The shaded region around the line of fit shows the confidence of fit. Micrographic measurements of the cross-sectioned microcapsules are provided as Supporting Information.

SiO_2 nanopowder emulsifier (Scheme 1 A). Similarly, DTS/BCI/GA refers to a DTS-filled microcapsule with a BCI shell and a Gum Arabic emulsifier (Scheme 1 B).

Quantification of Encapsulated IPDI and OTS. Fourier transform infrared (FTIR) spectroscopy was performed using a PerkinElmer Spectrum 100 spectrophotometer and an International Crystal Laboratories model SL-3 KBr liquid cell with a path length of 0.0986 mm. Concentrations of the components were determined using Beer's Law with the 1193 cm^{-1} peak assigned to OTS and the 2950 cm^{-1} peak assigned to IPDI. Samples were prepared by loading 250 mg of microcapsules and 10 mL of tetrachloroethylene into a 15 mL Ultraturrax grinding vessel and milling for 5 min. The solution was allowed to settle prior to extraction of 3 mL, which was then loaded into the KBr cell.

Gas chromatographic/mass spectrometry (GC/MS) analysis of the microcapsules was performed using a Shimadzu 17A with a tandem QP-5050A Electron Impact quadrupole mass spectral detector, equipped with a DB-5 capillary column. Microcapsule samples of 20 ± 2.0 mg were accurately weighed (Mettler-Toledo Model XP205) into a scintillation vial, suspended in 20 mL of acetone and placed into an ultrasonic bath (Crest Ultrasonics Model 230D) for 20 min. An aliquot was removed to a 2 mL sample vial, and 1 μL was injected into the GC/MS. Peak areas for each component were measured and quantified with an external standard. Note: the isocyanate components are comprised of isomers, so the individual peak areas were grouped together prior to quantification. Additional details of the GC/MS data analysis are provided as Supporting Information.

Effects of Synthesis Conditions on Glass Transition Temperature. To determine the glass transition temperature (T_g) of the microcapsules, dynamic mechanical analysis (DMA) was used. All microcapsules were first crushed and then pressed into thin disks of 12 mm in diameter and 2 mm in thickness using a Carver press under a force of 67 kN. Compression mode DMA tests were performed using a RSA-G2 analyzer from TA Instruments under an oscillating strain of 0.5% and an oscillating frequency of 1 Hz. Test samples were heated from −50 to 150 °C at a ramping rate of 3 °C/min and under a nitrogen atmosphere (99.9%). The T_g was determined according to ASTM E 1640.

Thermomechanical analysis (TMA) of T_g was performed using the PerkinElmer SII thermal mechanical analyzer. Prior to the test, all samples were pressed into 3 mm thick disc using a force of 67 kN. All samples were tested in compression mode with a preload of 200 mN to ensure good contact throughout the measurement. Samples were heated at a heating rate of 3 °C/min from −50 to 150 °C. T_g was then determined according ASTM E1545.

Effects of Temperature on OTS Hydrolysis. Aliquots (100 mg) of 65% OTS microcapsules were placed in water and heated to a fixed temperature for extended periods of time to measure the temperature dependence of hydrolysis. Five temperatures were used: 30, 35, 40, 45, and 50 °C. The OTS and IPDI concentrations were measured at each temperature periodically to record the amount of hydrolytic degradation using FTIR.

Effects of Solvent on OTS Leaching. Aliquots (20 mg) of 65% OTS microcapsules were immersed in 20 mL of an organic solvent for an extended period of time to determine the rate of OTS permeation through the microcapsule shell. The microcapsules were exposed to three different solvents, which were chosen to simulate the polarity of common solvent-reducible paint formulations: methylethylketone (MEK), xylenes, and hexanes. The experiment was performed at both room temperature and 40 °C for up to 80 days. GC recorded the concentration of OTS and IPDI in the supernatant at periodic intervals.

Microcapsule Mechanical Properties. The critical shear stress required for microcapsule rupture was initially tested using a Couette viscometer. It has a maximum speed of 24 000 rpm, the fluid has a 95 mm^2/s kinematic viscosity at 20 °C (35 mm^2/s viscosity at 40 °C), the cup diameter is 51 mm, and the bob diameter is 44 mm, giving a 7 mm gap. Because the Couette viscometer did not generate sufficient shear for microcapsule rupture, the microcapsules were subjected to further shear by spraying the microcapsules through a high-volume low-pressure (HVLP) spray gun. The microcapsules were sprayed through a Graco FX 3000 spray gun using a pressure of 206 kPa. Microcapsules (1% w/w) were added to silicone oil with viscosities of 100, 200, and 500 mm^2/s.

The effects of fluid shear on microcapsule rupture were tested in a more controlled fashion by vortexing a 1% (w/w) suspension of microcapsules in 500 mm^2/s silicone oil in a IKA Ultra-Turrax Tube Drive Workstation. The workstation was used together with the DT-20 tube with rotor-stator element. The stator has an inner diameter of 26 mm, the rotor has an outer diameter of 20 mm, and the circumferential speed is 6.5 m/s at 6000 rpm. The rotor-stator was operated at 6000 rpm for exactly 10 s on each 10 g sample. Afterward, the microcapsules were placed on a glass slide, coverslipped, and inspected under a light microscope.

Finally, individual microcapsules were tested under compression until rupture. Force and displacement were recorded with an Instron 5940 Series Single Column Tabletop System equipped with a 5 N load cell. Capsules were isolated on a 500 square micron piece of silicon wafer and tested at a head speed of 6 μm/min. Microcapsule diameters were measured prior to crush testing using a Zeta-20 optical profilometer. Microcapsule dynamics were observed with a camera equipped with a Scienscope MZ7A micro zoom lens during compression. The raw force and displacement data at failure were then converted into a rupture stress and rupture strain by assuming a spherical shape for the microcapsules. Thus, the force was normalized by the cross sectional area of the whole microcapsule, interior included, to calculate the stress, and the engineering strain was calculated by taking the change in height divided by the original diameter.

RESULTS AND DISCUSSION

Microcapsule Structure. Microscopic inspection revealed the average microcapsule diameter to be 23 ± 10 μm, which

DOI: 10.1021/acsami.5b00494
ACS Appl. Mater. Interfaces 2015, 7, 7315−7323

was roughly constant for all reaction conditions (Figure 1A). The size distribution of the emulsion prior to annealing in water was smaller, at 14 ± 7 μm. The larger, broader size distribution of the microcapsules implies that some emulsion droplets coalesce prior to interfacial polymerization. The shell thickness was estimated by embedding the microcapsules in epoxy and polishing until the shells were exposed in cross-section. With an average of 1.6 ± 0.6 μm, the shell thickness increased linearly with microcapsule diameter within the scatter of the data (Figure 1B). A linear relationship is expected for microcapsules with a constant mass fraction of isocyanate monomer that is completely consumed by the reaction. Representative scanning electron micrographs and the corresponding diagrams for the microcapsules are given in Scheme 2. Aside from a few silica agglomerates visible on the outer shell, the SiO_2-stabilized microcapsules were visually indistinguishable from Gum Arabic-stabilized microcapsules.

Scheme 2. Schematic of (A) a Gum Arabic-Stabilized Microcapsule (OTS/BCI/GA) and (B) a SiO_2-Stabilized Microcapsule (OTS/BCI/SiO_2) with Representative Scanning Electron Micrographs

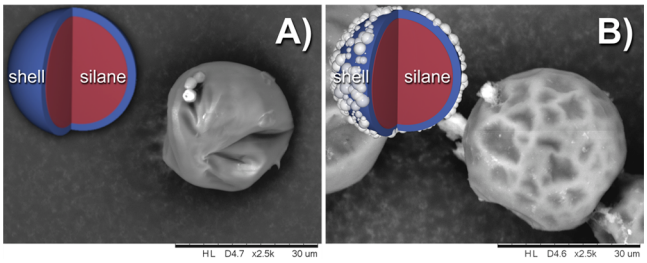

To verify that SiO_2 was taken up by the microcapsule, the microcapsule shells were analyzed via combustion analysis (Galbraith Laboratories, Knoxville, TN). Analysis for carbon, hydrogen, nitrogen, and silicon is conducted in an elemental analyzer that burns a small portion of sample in an oxygen atmosphere to create the combustion byproducts CO_2, H_2O, and N_2 (or NO_x). The gases are then separated and quantified by either an infrared cell or a thermal conductivity detector. Results are reported in weight fraction of the corresponding element. Si content was quantified by digesting the samples in aqueous HF solution and then performing inductively coupled plasma atomic emission spectroscopy (ICP-AES). Table 1

Table 1. Elemental Combustion Analysis of OTS/BCI/SiO_2 Microcapsules Processed at 90°C[a]

	DETA	IPDI	SiO_2	measured	fitted
C	0.47	0.65	0.00	0.58	0.57
H	0.13	0.08	0.00	0.09	0.07
N	0.41	0.13	0.00	0.12	0.12
Si	0.00	0.00	0.47	0.05	0.05

[a]The data fit indicates that the microcapsule shell consists of 11% SiO_2, 84% IPDI, and 4% DETA by weight.

shows that a reasonable fit to the measured data could be achieved by assuming that the shell was primarily composed of 84% IPDI, 4% DETA, and 11% SiO_2 by weight. The nitrogen fraction is much lower than expected on the basis of stoichiometry but is nevertheless consistent with other experiments that showed that polymer shell grows readily in pure water. Taken together, these data suggest that water may be more responsible for the polymerization of IPDI than DETA or PEI due to the greater diffusion rate through the growing polymer shell.

Interfacial Polymerization Kinetics. The formation of the polymer shell was monitored through the disappearance of the isocyanate peak from the liquid extracted from the microcapsules. The mass fractions of silane and isocyanate monomer are given for different formulations, incubation temperatures, and incubation times in Figure 2. In general, the OTS concentration did not change greatly from the initial feed concentration despite extensive exposure to water. The lone exceptions were the Gum Arabic stabilized microcapsules at 90 °C. The result shows that the polyurea shell cannot protect the OTS from hydrolysis at elevated temperatures. Notably, the SiO_2-stabilized microcapsules preserved nearly all of the original OTS under the same conditions. Further evidence of the SiO_2 barrier properties can be seen in the decreased rate of interfacial polymerization. In contrast to Gum Arabic, SiO_2-stabilized microcapsules could not be produced at room temperature after 2 weeks.

The data also show that the BCI reacts more slowly than IPDI. This observation likely arises because BCI has two secondary isocyanates, whereas IPDI has one secondary isocyanate and one primary isocyanate, the latter of which exhibits greater reactivity.[30]

Shelf Life. Real-time aging experiments were performed on a large set of OTS/IPDI/SiO_2 batches under ambient conditions to determine the shelf life of OTS entrained within the microcapsules. Figure 3 shows that the hydrolytic degradation of OTS was negligible over the course of 4 months. Also note the large standard deviation. In addition to the difficulty of tracking such small changes in mass, the relatively large error may also stem from batch-to-batch variations and OTS reacting with metal or glass surfaces during the measurement process. IPDI, on the other hand, gave more reliable values for mass loss. The data imply that IPDI preferentially reacted with the water that diffused into the microcapsule on account of its higher reactivity relative to OTS. A linear regression fit to the data estimates that IPDI is lost at a rate of only 0.2% (w/w) per month.

Similar measurements were repeated for a number of microcapsule variations to better understand the effects of the silica nanopowder, the polymer shell, and the polarity of the fill. Microcapsules were made using either SiO_2 nanopowder or Gum Arabic as an emulsifier to compare the silica composite shell versus a pure polymer shell. The polymer shell was made using either IPDI or BCI to compare the effects of the polymer shell composition on the barrier properties. Finally, OTS was swapped with DTS to see if the slightly more polar DTS had a significant impact on the quality of the polymer shell and, hence, the resultant barrier properties. For this comparison, all microcapsules were incubated at 60 °C for 4 days.

Figure 4 shows that the effects of the fill polarity were minimal. The OTS-filled microcapsules did not consistently perform better than the DTS-filled microcapsules, except when Gum Arabic was the emulsifier. One would not expect a large difference between OTS and DTS because the difference in polarity is small. Most pronounced was the difference between the SiO_2-coated and uncoated polymer shells. The rate of loss of IPDI went from −4%/mo. to −0.1%/mo. upon the addition SiO_2 filler. This decrease in hydrolysis rate can be explained in terms of the tortuous diffusion path that the water must take

DOI: 10.1021/acsami.5b00494
ACS Appl. Mater. Interfaces 2015, 7, 7315−7323

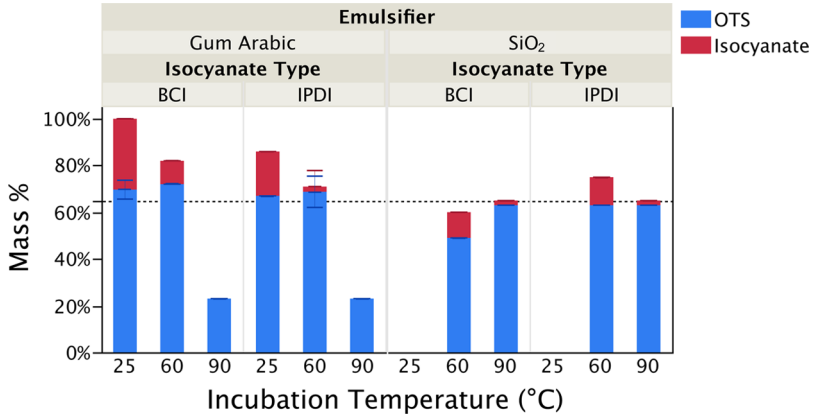

Figure 2. Average of gas chromatography and FTIR measurements for the mass fraction of OTS and isocyanate monomer under different incubation temperatures, monomer types, and emulsifiers. Note that SiO_2-stabilized microcapsules did not form after 2 weeks at room temperature. The error bars show the standard deviation, and the dashed line indicates the initial concentration of OTS in the feedstock. Photographs of each batch of microcapsules are provided in the Supporting Information.

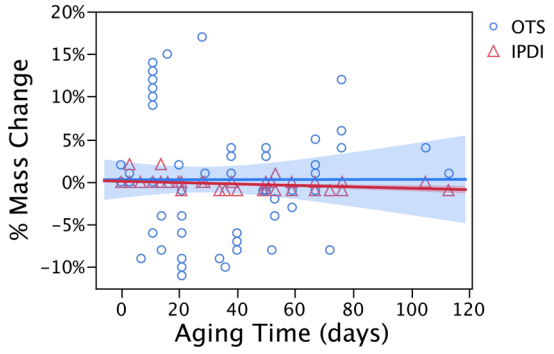

Figure 3. Gas chromatography measurements of the change in mass of OTS and IPDI as a function of time for a large number of OTS/IPDI/SiO_2 microcapsule batches under ambient conditions. The shaded regions highlight the confidence of fit.

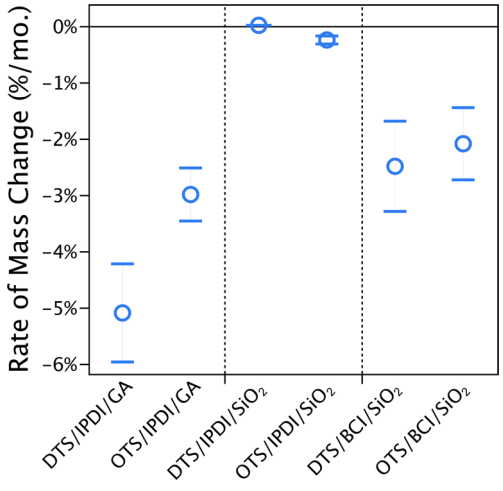

Figure 4. Rate of isocyanate mass change per month, calculated from linear regression fits, is plotted for each sample type with error bars representing the standard deviation. The mass change of silane per month (not shown) hovered near zero with a large standard deviation.

through the silica-filled polymer matrix in order to reach the unreacted IPDI at the center of the microcapsule.

The effects of the shell-forming monomer were also significant. Switching from IPDI to BCI nearly reversed the gains from adding the SiO_2 nanopowder. This finding suggests that the BCI shells might be more permeable to water. Figure 5

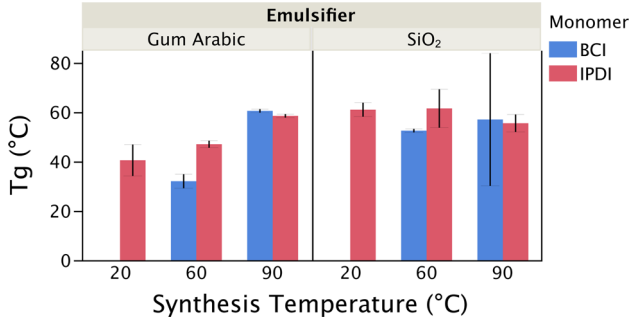

Figure 5. Glass transition temperature is plotted for the microcapsule shell for different synthesis temperatures, emulsifiers, and monomer types. The error bars show the standard deviation.

shows that the glass transition temperature (T_g) is lower for BCI than IPDI when the microcapsules are synthesized at 60 °C. The lower T_g suggests the BCI shell may be more lightly cross-linked or have greater chain mobility, both of which could explain the greater permeability to water.[31] The T_g also decreased in the absence of the SiO_2 nanopowder, which means that a similar argument could be made for the increased permeability of the Gum Arabic microcapsules. It is not clear why the SiO_2 nanopowder would affect chain mobility or cross-link density, but the measured increase in T_g was significant.

Further inspection of aging data for a batch of OTS/BCI/SiO_2 microcapsules reveals an additional culprit for the reduced shelf life of the BCI microcapsules (Figure 6). Observe how both BCI and OTS decrease in concentration. Previously, only IPDI decreased in concentration and OTS stayed constant. A possible explanation is that the reduced reactivity of BCI with water makes it comparable to OTS. Whereas water reacts preferentially with IPDI, it has a significant probability of reacting with OTS in the presence of BCI. This finding highlights an easily overlooked role of the shell-forming monomer. It needs to react preferentially with water and cross-linkers during interfacial polymerization, but residual monomer might also act as a water scavenger to bolster the shelf life of the active ingredient once synthesis has completed.

DOI: 10.1021/acsami.5b00494
ACS Appl. Mater. Interfaces 2015, 7, 7315−7323

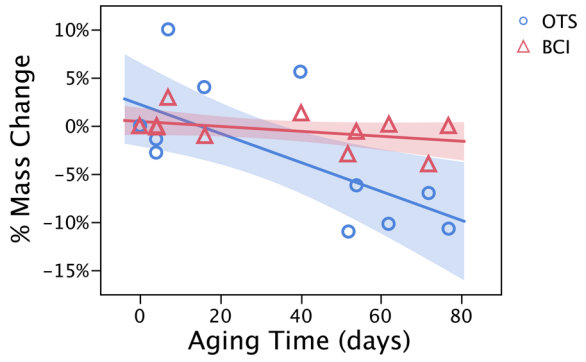

Figure 6. Gas chromatography measurements of the change in mass of OTS and BCI as a function of time for several batches of OTS/IPDI/SiO_2 microcapsules under ambient conditions. The shaded areas highlight the confidence of fit.

To study the kinetics of hydrolysis in greater detail, we repeated the same experiments by immersing the OTS/IPDI/SiO_2 microcapsules in water at elevated temperature. Pseudo-first order reaction kinetics was assumed by ignoring the small changes in water concentration and shell thickness. The rate of hydrolysis would thus be given by $-d[A]/dt = k[A]$, where $[A]$ is the molar concentration of the reagent, t is time, and k is the reaction rate constant. In agreement with Figure 3, Figure 7

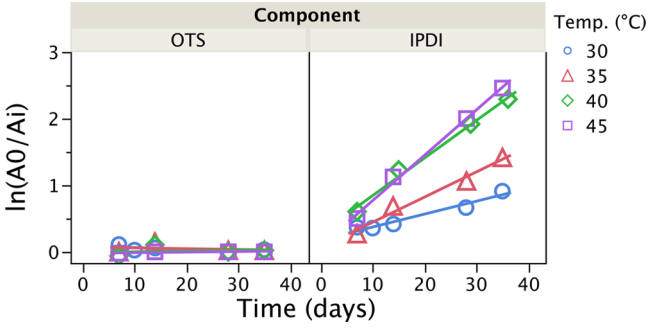

Figure 7. Natural log of the initial concentration divided by final concentration is plotted versus time for both OTS and IPDI in the OTS/IPDI/SiO_2 sample. The linear fits show that the OTS concentration is largely invariant during the time frame of the experiment, while the IPDI concentration has an exponential relationship with time in accordance with pseudo-first-order reaction kinetics.

shows that IPDI again proved to be the more reliable indicator of hydrolysis. The linear fits to $\ln(A_0/A_i)$ versus t show that the consumption of IPDI is, in fact, consistent with pseudo first order kinetics under these conditions.

For interfacial polymerization reactions in microcapsules, the rate of monomer conversion is controlled by the diffusion of reactants across the polymer barrier layer.[32−34] In such cases, k is directly proportional to the diffusion coefficient.[35−37] The temperature dependence therefore usually corresponds to the activation energy of water diffusion rather than the reaction between water and isocyanate. The Arrhenius plot in Figure 8 assigns a value of 48 kJ/mol for the activation energy (ΔE_a) of OTS/IPDI/SiO_2 and 82 s^{-1} for k_0. For OTS/IPDI/GA, ΔE_a comes out to 82 kJ/mol and k_0 is 1.5×10^8 s^{-1}. As expected, SiO_2 reduced k_0 due to the more tortuous path for water diffusion, but the decrease in ΔE_a is intriguing. One might not expect any change in ΔE_a since the diffusion of water should

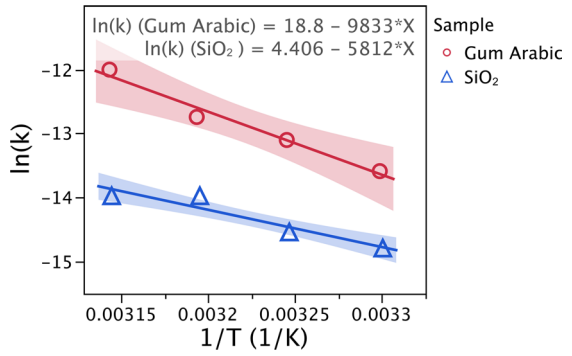

Figure 8. Arrhenius plot for IPDI hydrolysis comparing OTS/IPDI/SiO_2 to OTS/IPDI/GA. The slope of the lines give an activation energy of 48 kJ/mol for OTS/IPDI/SiO_2 and 82 kJ/mol for OTS/IPDI/GA. The intercepts give $k_0 = 82$ s^{-1} for OTS/IPDI/SiO_2 and $k_0 = 1.5 \times 10^8$ s^{-1} for OTS/IPDI/GA. The shaded areas highlight the confidence of fit.

still largely occur through the same polyurea in both cases. Figure 5 does show, however, that the T_g is much different for these two polymers. In the case of OTS/IPDI/GA, it actually goes through T_g at 47 °C, which is very close to the range of test conditions. Plasticization by water could have easily depressed T_g below some of the measurement temperatures. If true, then the apparent increase in activation energy for OTS/IPDI/GA could be due to the OTS/IPDI/GA microcapsule being in the rubbery rather than glassy state. Though counterintuitive, free volume theory predicts that ΔE_a goes through a discontinuous jump above T_g.[38,39] Near T_g, ΔE_a can therefore be higher in the rubbery state, in agreement with the data. Keep in mind, however, that the difference between the two ΔE_a values lies within experimental error. Nevertheless, the experiments show that microcapsules synthesized with SiO_2 nanopowder exhibit vastly improved resistance toward hydrolysis.

Solvent Resistance. The barrier properties of the microcapsules were also tested with respect to solvent resistance. For these experiments, the microcapsules were immersed in solvents with low (hexanes), moderate (xylenes), and high (MEK) polarities. GC then recorded the quantity of OTS that leached into the supernatant. Figure 9 shows that the extraction of OTS occurred rapidly in MEK for OTS/IPDI/SiO_2 and the OTS/BCI/SiO_2. Similar results occurred for ethanol and

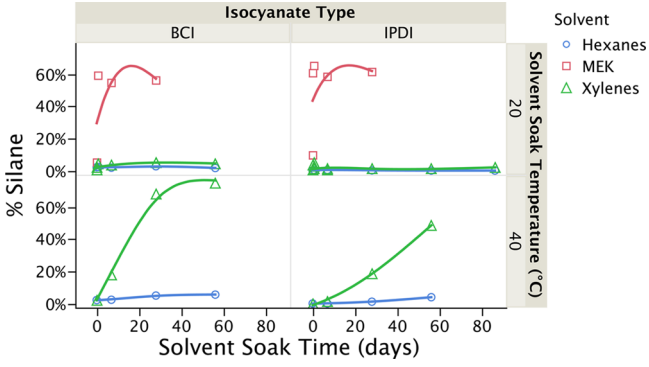

Figure 9. Mass fraction of silane detected in the solvent by gas chromatography is plotted as a function of time for SiO_2-stabilized BCI and IPDI microcapsules (OTS/BCI/SiO_2 and OTS/IPDI/SiO_2) tested at 20 and 40 °C.

DOI: 10.1021/acsami.5b00494
ACS Appl. Mater. Interfaces 2015, 7, 7315−7323

acetone. Despite being insoluble in these solvents, the polymers formed from BCI and IPDI appear to at least swell with polar organic solvents. We hypothesize that the hydrogen-bonding capability of these solvents may be competing with intramolecular hydrogen bonds within the polyurea. Note that no microcapsule rupture was observed. The swelling then increases the permeability of OTS through the polymer. Both IPDI and BCI microcapsules released the entirety of the OTS within 24 h.

Hexanes, in contrast, caused almost no leaching of OTS. Only when the temperature increased to 40 °C was the amount of leached OTS significant. Even then it was below 5%. Xylenes caused slightly more leaching. At room temperature, it amounted to 5% OTS for BCI after 50 days and 2% OTS for IPDI after 80 days. At 40 °C, about 50% diffused out of the IPDI microcapsules after 50 days and 60% leached out of the BCI microcapsules after 30 days. Here again, note the improved barrier properties of the IPDI-based polyurea relative to the BCI-polyurea.

When comparing OTS/IPDI/GA microcapsules and OTS/IPDI/SiO_2 microcapsules, the effects of the SiO_2 composite are more pronounced here as well (Figure 10). Over the course of 28 days, the amount of OTS leached into the solvent was roughly 4× greater without the silica reinforcement.

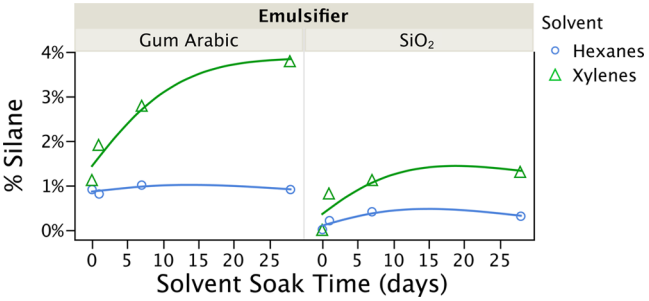

Figure 10. Mass fraction of silane detected in the solvent by gas chromatography is plotted as a function of time for OTS/IPDI/GA, and OTS/IPDI/SiO_2 microcapsules.

Rupture Stress. The OTS/IPDI/SiO_2 microcapsules did not rupture in the Couette viscometer despite a 95 mm^2/s viscosity and a rotation speed of 24 000 rpm (2513 rad/s). To obtain an idea of how greatly the microcapsules exceeded the maximum applied shear stress, we intentionally synthesized weaker microcapsules by incubating them for shorter times in water. So rather than 1 day at 90 °C, the microcapsules were incubated for 4, 8, 16, 20, and 24 h to obtain thinner shells. Only a small fraction of the 4 h microcapsules broke, even at 24 000 rpm. About 7% of the microcapsules broke at that speed according to post-test microscopic inspection.

Because the microcapsules experience the greatest stresses during spray painting, the microcapsules were sprayed from a spray paint nozzle in a viscous fluid at high pressure. For these experiments, viscous silicone oil created shear conditions that greatly exceeded those expected from a typical paint. 100, 200, and 500 cSt silicone oils were tested. The 206 kPa pressure was similarly chosen to challenge the microcapsule shells. Here again the OTS/IPDI/SiO_2 microcapsules did not break under any conditions. However, a fraction of the OTS/IPDI/GA microcapsules did rupture in the 500 cSt silicone oil, demonstrating a clear improvement in mechanical properties due to the silica nanoparticle filler.

The effects of fluid shear on microcapsule rupture were further investigated by vortexing a 1% (w/w) suspension of microcapsules in 500 mm^2/s silicone oil in a rotor-stator at 6000 rpm. Figure 11 presents micrographs of the microcapsules

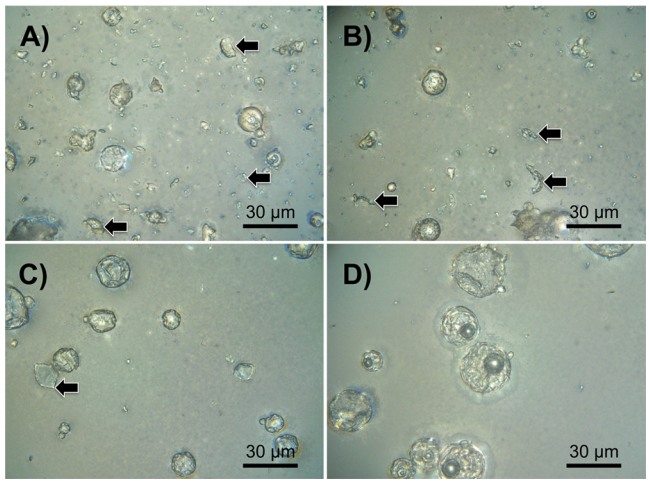

Figure 11. Micrographs of microcapsules in 500 mm^2/s silicone oil after 60 s of vortexing in a rotor-stator at 6000 rpm for A) OTS/IPDI/GA, B) OTS/BCI/GA, C) OTS/IPDI/SiO_2, and D) OTS/IPDI/SiO_2. Arrows indicate locations with shell fragments.

after 60 s of shear. Observe the extent of microcapsule debris for the microcapsules stabilized with Gum Arabic. Both OTS/IPDI/GA and OTS/BCI/GA experienced extensive microcapsule fragmentation under these conditions. However, one confounding factor in this observation is the fact that microcapsule agglomeration may have contributed to the extent of debris.

The silica-stabilized microcapsules, in contrast to the pure polymer microcapsules, withstood the shear conditions of the rotor-stator. The OTS/IPDI/SiO_2 showed only minor evidence of microcapsule rupture, and OTS/IPDI/GA showed none. Although the BCI microcapsules generally exhibited worse shelf life and solvent resistance relative to IPDI microcapsules, they appear to be somewhat stronger mechanically. Compression tests of individual microcapsules support this observation. Figure 12 shows that the OTS/BCI/SiO_2 microcapsules had roughly triple the rupture stress and strain compared to those of OTS/IPDI/SiO_2.

CONCLUSION

The addition of SiO_2 nanopowder caused significant improvements in rupture strength, solvent resistance, and moisture barrier properties. The effects of the SiO_2 filler were greater than those obtained by altering the polymer chemistry or the polarity of the fill. The results support our initial hypothesis that the SiO_2 filler provides mechanical reinforcement to the shell and inhibits the diffusion of water and organic molecules through the shell. Perhaps equally important are the implications to the microcapsule synthesis; the greater emulsion stability made it possible to incubate the microcapsules at higher temperature, and the incorporation of the SiO_2 into the shell eliminated the need for purification.

DOI: 10.1021/acsami.5b00494
ACS Appl. Mater. Interfaces 2015, 7, 7315−7323

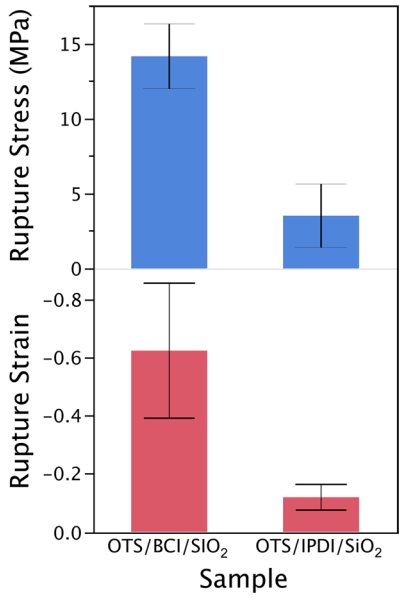

Figure 12. Rupture stress and rupture strain of individual microcapsules plotted for OTS/BCI/SiO_2 and OTS/IPDI/SiO_2. Error bars show the standard deviation.

■ ASSOCIATED CONTENT

Ⓢ Supporting Information

Additional photographs of the bulk microcapsule samples after processing illustrating the improvement in sample quality afforded by the addition of silica nanopowder as an emulsifying agent and additional information for the gas chromatography technique used to quantify the mass fraction of remaining OTS and isocyanate monomer within the microcapsules. This material is available free of charge via the Internet at http://pubs.acs.org.

■ AUTHOR INFORMATION

Corresponding Author

*E-mail: jason.benkoski@jhuapl.edu.

Notes

The authors declare no competing financial interest.

■ ACKNOWLEDGMENTS

We thank the Office of Naval Research for financial support. This research was funded by ONR Code 30 Logistics Thrust under grant no. N00014-09-1-0383. We also thank the Program Management Office for Light Tactical Vehicles of the U.S. Marine Corps for their overall support of this program.

■ REFERENCES

(1) Tsuji, K. Microencapsulation of Pesticides and their Improved Handling Safety. *J. Microencapsulation* **2001**, *18*, 137−147.
(2) Shukla, P. G.; Kalidhass, B.; Shah, A.; Palakar, D. V. Preparation and Characterization of Microcapsules of Water-Soluble Pesticide Monocrotophos using Polyurethane as Carrier Material. *J. Microencapsulation* **2002**, *19*, 293−304.
(3) Hong, K.; Park, S. Melamine Resin Microcapsules Containing Fragrant Oil: Synthesis and Characterization. *Mater. Chem. Phys.* **1999**, *58*, 128−131.
(4) White, M. A. The Chemistry Behind Carbonless Copy Paper. *J. Chem. Educ.* **1998**, *75*, 1119−1120.
(5) Rutledge, L. C.; Gupta, R. K. Evaluation of Controlled-Release Mosquito Repellent Formulations. *J. Am. Mosq. Control Assoc.* **1996**, *23*, 39−44.
(6) Beyger, J. W.; Nairn, J. G. Some Factors Affecting the Microencapsulation of Pharmaceuticals with Cellulose Acetate Phthalate. *J. Pharm. Sci.* **2006**, *75*, 573−578.
(7) Polk, A.; Amsden, B.; De Yao, K.; Peng, T.; Goosen, M. F. A. Controlled release of albumin from chitosan-alginate microcapsules. *J. Pharm. Sci.* **2006**, *83*, 178−185.
(8) Chang, T. M. S.; Poznansky, M. J. Semipermeable Aqueous Microcapsules (Artificial Cells). V. Permeability Characteristics. *J. Biomed. Res.* **2004**, *2*, 187−199.
(9) Brissová, M.; Petro, M.; Lacík, I.; Powers, A. C.; Wang, T. Evaluation of Microcapsule Permeability via Inverse Size Exclusion Chromatography. *Anal. Biochem.* **1996**, *242*, 104−111.
(10) Chang, T. M. Biodegradable Semipermeable Microcapsules Containing Enzymes, Hormones, Vaccines, and Other Biologicals. *J. Bioeng.* **1976**, *1*, 25−32.
(11) Johnston, A. P. R.; Cortez, C.; Angelatos, A. S.; Caruso, F. Layer-by-Layer Engineered Capsules and their Applications. *Curr. Opin. Colloid Interface Sci.* **2006**, *11*, 203−209.
(12) Freiberg, S.; Zhu, X. X. Polymer Microspheres for Controlled Drug Release. *Int. J. Pharm.* **2004**, *282*, 1−18.
(13) Lensen, D.; Gelderblom, E. K.; Vriezema, D. M.; Marmottant, P.; Verdonschot, N.; Versluis, M.; de Jong, N.; van Hest, J. C. M. Biodegradable Polymeric Microcapsules for Selective Ultrasound-Triggered Drug Release. *Soft Matter* **2011**, *7*, 5417−5422.
(14) Chang, M.-W.; Edirisinghe, M.; Stride, E. Ultrasound Mediated Release from Stimuli-Responsive Core-Shell Capsules. *J. Mater. Chem. B* **2013**, *1*, 3962−3971.
(15) Liu, L.; Wang, W.; Ju, X.-J.; Xie, R.; Chu, L.-Y. Smart Thermo-Triggered Squirting Capsules for Nanoparticle Delivery. *Soft Matter* **2010**, *6*, 3759−3763.
(16) Yeo, Y.; Bellas, E.; Firestone, W.; Langer, R.; Kohane, D. S. Complex Coacervates for Thermally Sensitive Controlled Release of Flavor Compounds. *J. Agric. Food Chem.* **2005**, *53*, 7518−7525.
(17) Pastine, S. J.; Okawa, D.; Zettl, A.; Fréchet, J. M. J. Chemicals on Demand with Phototriggerable Microcapsules. *J. Am. Chem. Soc.* **2009**, *131*, 13586−13587.
(18) San Miguel, A.; Scrimgeour, J.; Curtis, J. E.; Behrens, S. H. Smart Colloidosomes with a Dissolution Trigger. *Soft Matter* **2010**, *6*, 3163−3166.
(19) Hertzberg, R. W. *Deformation and Fracture Mechanics of Engineering Materials*, 4th ed; John Wiley & Sons, Inc.: New York, NY, 1996.
(20) Brannon-Peppas, L., In *Polymeric Delivery Systems: Properties and Applications, ACS Symposium Series 520*, 4th ed; M. A. El-Nokaly, Piatt, D.M.; Charpentier, B.A., Eds.; American Chemical Society: Washington, DC, 1993; pp 42−52.
(21) Wang, Z. F.; Wang, B.; Qi, N.; Zhang, H. F.; Zhang, L. Q. Influence of Fillers on Free Volume and Gas Barrier Properties in Styrene-Butadiene Rubber Studied by Positrons. *Polymer* **2005**, *46*, 719.
(22) Kaiser, A.; Liu, T.; Richtering, W.; Schmidt, A. M. Magnetic Capsules and Pickering Emulsions Stabilized by Core−Shell Particles. *Langmuir* **2009**, *25*, 7335−7341.
(23) Bon, S. A. F.; Chen, T. Pickering Stabilization as a Tool in the Fabrication of Complex Nanopatterned Silica Microcapsules. *Langmuir* **2007**, *23*, 9527−9530.
(24) McIlroy, D. A.; Blaiszik, B. J.; Caruso, M. M.; White, S. R.; Moore, J. S.; Sottos, N. R. Microencapsulation of a Reactive Liquid-Phase Amine for Self-Healing Epoxy Composites. *Macromolecules* **2010**, *43*, 1855−1859.
(25) van Wijk, J.; Salari, J. W. O.; Zaquen, N.; Meuldijk; Klumperman, B. Poly(methyl methacrylate)-Silica Microcapsules Synthesized by Templating Pickering Emulsion Droplets. *J. Mater. Chem. B* **2013**, *1*, 2394−2406.
(26) Binks, B. P. Particles as Surfactants—Similarities and Differences. *Curr. Opin. Colloid Interface Sci.* **2002**, *7*, 21−41.
(27) Fielding, L. A.; Armes, S. P. Preparation of Pickering Emulsions and Colloidosomes using either a Glycerol-Functionalised Silica Sol or

DOI: 10.1021/acsami.5b00494
ACS Appl. Mater. Interfaces 2015, 7, 7315−7323

Core−Shell Polymer/Silica Nanocomposite Particles. *J. Mater. Chem.* **2012**, *22*, 11235−11244.
(28) Yang, Y.; Wei, Z.; Wang, C.; Tong, Z. Versatile Fabrication of Nanocomposite Microcapsules with Controlled Shell Thickness and Low Permeability. *ACS Appl. Mater. Interfaces* **2013**, *5*, 2495−2502.
(29) Wu, G.; An, J.; Sun, D.; Tan, X.; Xiang, Y.; Yang, J. Robust Microcapsules with Polyurea/Silica Hybrid Shell for One-Part Self-Healing Anticorrosion Coatings. *J. Mater. Chem. A* **2014**, *2*, 11614−11620.
(30) Lomölder, R.; Plogmann, R.; Speier, P. Selectivity of Isophorone Diisocyanate in the Urethane Reaction Influence of Temperature, Catalysis, and Reaction Partners. *J. Coat. Technol.* **1997**, *69*, 51−57.
(31) Neogi, P. *Diffusion in Polymers*; Marcel Dekker, Inc.: New York, 1996, Ch 3.
(32) Pearson, R. G. Interfacial Polymerization of an Isocyanate and a Diol. *J. Polym. Sci., Polym. Chem. Ed.* **1985**, *23*, 9−18.
(33) Morgan, P. W.; Kwolek, S. L. Interfacial Polycondensation. II. Fundamentals of Polymer Formation at Liquid Interfaces. *J. Polym. Sci.* **1959**, *40*, 299−327.
(34) MacRitchie, F. Mechanism of Interfacial Polymerization. *Trans. Faraday Soc.* **1968**, *65*, 2503−2507.
(35) Khawam, A.; Flanagan, D. R. Solid-State Kinetic Models: Basics and Mathematical Fundamentals. *J. Phys. Chem. B* **2006**, *110*, 17315−17328.
(36) Jander, W. Reactions in the Solid State at High Temperature. *Z. Anorg. Allg. Chem.* **1927**, *163*, 1−30.
(37) Ginstling, A. M.; Brounshtein, B. T. Reactions in the Solid State at High Temperature. *J. Appl. Chem. USSR* **1950**, *23*, 1328−1338.
(38) Vrentas, J. S.; Duda, J. L. A Free-Volume Interpretation of the Influence of the Glass Transition Temperature on Diffusion in Amorphous Polymers. *J. Appl. Polym. Sci.* **1978**, *22*, 2325−2339.
(39) Romdhane, I. H.; Danner, R. P.; Duda, J. L. Influence of the Glass Transition on Solute Diffusion in Polymers by Inverse Gas Chromatography. *Ind. Eng. Chem. Res.* **1995**, *34*, 2833−2840.

DOI: 10.1021/acsami.5b00494
ACS Appl. Mater. Interfaces 2015, 7, 7315−7323